34th Annual International Conference of the IEEE EMBS
San Diego, California USA, 28 August - 1 September, 2012

Training Strategies for a Lower Limb Rehabilitation Robot Based on Impedance Control*

Jin Hu, Zengguang Hou, Feng Zhang, Yixiong Chen and Pengfeng Li

***Abstract*— This paper proposes three training strategies based on impedance control, including passive training, damping-active training and spring-active training, for a 3-DOF lower limb rehabilitation robot designed for patients with paraplegia or hemiplegia. Controllers with similar structure are developed for these training strategies, consisting of dual closed loops, the outer impedance control loop and the inner position/velocity control loop, known as position-based impedance control method. Simulation results verify that position-based impedance control approach is feasible to accomplish the training strategies.**

I. Introduction

Plenty of common diseases and accidents may lead to paraplegia or hemiplegia, accordingly, the number of these patients is growing huge. Compared to traditional physiotherapy, rehabilitation robot can reduce the cost. Besides, it can provide various training strategies, broadly classified into passive training and active training, which both have been proven effective to rehabilitation by clinic trials [1], [2], [3].

During rehabilitation training, affected limbs are required direct contact with robot. For the benefit of security, force control for rehabilitation robot has to be considered. The most extensively used approach is impedance control.

Y. Yang et al. proposed a position-based impedance control method for an arm rehabilitation robot to achieve a certain compliance and security during passive training [4]. E. G. Cao et al. adopted an impedance control approach for a sit-to-stand trainer system in lower limb rehabilitation to assure that patients safely and effectively stood up in their normal and comfortable posture [5]. An impedance control law was also employed in [6] to a 3-DOF upper limb rehabilitation robot in human-robot interactions for its advantages in term of safety to fulfill two of the rehabilitation modes.

Overall, impedance control used for rehabilitation robot mainly focus on compliant behavior, and there is little literature involving elaborate training strategies on the basis of impedance control. In this study, training strategies using position-based impedance control for a 3-DOF lower limb rehabilitation robot designed for patients with paraplegia or hemiplegia are more elaborately described.

*This work is supported in part by National Natural Science Foundation of China (Grant #61175076) and by Sci. & Tech. Program for Supervisor of the Recipient of Outstanding Doctorate Dissertation of Beijing (Grant #YB20108000103)

Jin Hu, Zengguang Hou, Feng Zhang, Yixiong Chen and Pengfeng Li are with State Key Laboratory of Management and Control for Complex Systems, Institute of Automation, Chinese Academy of Sciences, Beijing 100190, China ustbhujin@163.com, hou@compsys.ia.ac.cn, zfeng1203@yahoo.com.cn, yourfriendcyx@163.com, lipengfeng007@163.com

II. Lower Limb Rehabilitation Robot

The mechanical structure of the 3-DOF exoskeleton robot for lower limb rehabilitation is shown in Fig. 1. Three joints correspond to hip joint, knee joint and ankle joint of a lower limb. An absolute encoder, a relative encoder and a torque sensor are installed at each joint to record the joint angle, angular velocity and torque, respectively. During rehabilitation training, lower limb is attached to the robot, and the entire system, robot together with the lower limb attached, can be considered as a three-link structure. For simplicity, it is assumed that the mass of the system is evenly distributed, and the second joint below is treated as a single link, since the third joint and link have little influence on the end-point trajectory. Therefore, the simplified model of the system is a two-link structure shown in Fig. 2.

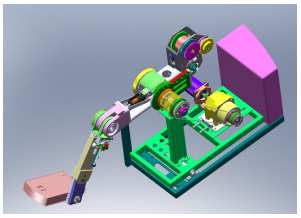

Fig. 1. Mechanical structure of rehabilitation robot

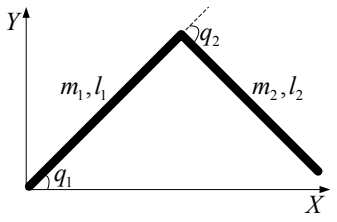

Fig. 2. Simplified structure of system

A. Kinematic Analysis

From Fig. 2, forward kinematics of the system can be directly deduced as

$$\begin{bmatrix} x \\ y \end{bmatrix} = \begin{bmatrix} l_1 \cos q_1 + l_2 \cos(q_1 + q_2) \\ l_1 \sin q_1 + l_2 \sin(q_1 + q_2) \end{bmatrix} \tag{1}$$

where l_1, l_2 represent the length of link 1 and that of link 2 respectively, and q_1, q_2 represent the angle of joint 1 and that of joint 2, and x, y represent the end-point position in Cartesian space coordinates. Inverse kinematics can be derived from (1), under the constraint that $q_2 < 0$, represented as

$$\begin{bmatrix} q_2 \\ q_1 \end{bmatrix} = \begin{bmatrix} -\arccos \frac{x^2+y^2-l_1^2-l_2^2}{2l_1l_2} \\ \arcsin \frac{y}{\sqrt{x^2+y^2}} - \arctan \frac{l_2 \sin q_2}{l_1+l_2 \cos q_2} \end{bmatrix}. \tag{2}$$

By differentiating (1), Jacobian matrix can be written as

$$J = \begin{bmatrix} -l_1 \sin q_1 - l_2 \sin(q_1 + q_2) & -l_2 \sin(q_1 + q_2) \\ l_1 \cos q_1 + l_2 \cos(q_1 + q_2) & l_2 \cos(q_1 + q_2) \end{bmatrix}. \tag{3}$$

If $q_2 = 0$, $\det(J) = 0$, i.e. $\text{rank}(J) < 2$, making the system in singular configurations, which should be avoided by setting

q_2 in a reasonable range in training strategies. Therefore, the inverse velocity kinematics can be expressed as $\dot{q} = J^{-1}\dot{X}$.

B. Dynamic Analysis

The application of Euler-Lagrange equations leads to ideal dynamic model of the system, given by the standard form as

$$D(q)\ddot{q} + C(q,\dot{q})\dot{q} + G(q) = \tau \tag{4}$$

where q, $\dot{q}$, $\ddot{q}$ are the vectors of joint angles, angular velocities and angular accelerations respectively, $D(q)$ is the symmetric positive-definite inertia matrix, $C(q,\dot{q})\dot{q}$ is the vector of Coriolis and centrifugal torques, $G(q)$ is the vector of gravitational torques, and τ is the vector of actuator joint torques. The matrix $\dot{D}(q) - 2C(q,\dot{q})$ is skew-symmetric, and the inertia matrix $D(q)$ is bounded [7], [8], [9]. $D(q)$, $C(q,\dot{q})$ and $G(q)$ are expressed by (5), (6) and (7) respectively.

$$\begin{cases} D_{11} = (\frac{1}{3}m_1 + m_2)l_1^2 + \frac{1}{3}m_2 l_2^2 + m_2 l_1 l_2 \cos q_2 \\ D_{12} = D_{21} = \frac{1}{3}m_2 l_2^2 + \frac{1}{2}m_2 l_1 l_2 \cos q_2 \\ D_{22} = \frac{1}{3}m_2 l_2^2 \end{cases} \tag{5}$$

$$\begin{cases} C_{11} = -\frac{1}{2}m_2 l_1 l_2 \dot{q}_2 \sin q_2 \\ C_{12} = -\frac{1}{2}m_2 l_1 l_2 (\dot{q}_1 + \dot{q}_2) \sin q_2 \\ C_{21} = \frac{1}{2}m_2 l_1 l_2 \dot{q}_1 \sin q_2 \\ C_{22} = 0 \end{cases} \tag{6}$$

$$\begin{cases} G_1 = (\frac{1}{2}m_1 + m_2)\mathrm{g} l_1 \cos q_1 + \frac{1}{2}m_2 \mathrm{g} l_2 \cos(q_1 + q_2) \\ G_2 = \frac{1}{2}m_2 \mathrm{g} l_2 \cos(q_1 + q_2) \end{cases} \tag{7}$$

where D_{ij} and C_{ij} denote the $(i,\ j)$ elements of $D(q)$ and $C(q,\dot{q})$ respectively, G_i denotes the i-th element of $G(q)$, and $m_1,\ m_2$ represent the mass of link 1 and that of link 2 respectively.

Dynamic model which takes friction, disturbance and human effect into account is rewritten as

$$D(q)\ddot{q} + C(q,\dot{q})\dot{q} + G(q) + T = \tau - \tau_h \tag{8}$$

where T is the vector of joint friction and external disturbance torques and τ_h is the vector of joint torques exerted on the robot by human.

III. Impedance Control and Training Strategies

Three training strategies, referred to as passive training, damping-active training and spring-active training, are proposed for the lower limb rehabilitation robot. Controllers with similar architecture are developed for these training strategies, named position-based impedance control approach, composed of dual closed loops. The outer impedance control loop is established for different purposes in different strategies. The inner position/velocity control loop is accomplished by statics-compensation-based PID algorithm with limited output, and the statics compensation is implemented by offline trained RBF artificial neural networks.

The position-based impedance control approach is employed to accomplish the training strategies in this study. The aim is to establish a desired relationship between the position and the force, called impedance function, expressed by the mass-damper-spring model as

$$F_e = M\ddot{X}_a + B\dot{X}_a + KX_a \tag{9}$$

where M, B and K are inertia, damping and stiffness coefficient matrices respectively. X_a, $\dot{X}_a$ and $\ddot{X}_a$ are the position, velocity and acceleration adjustments to the reference trajectory respectively and F_e is the contact force between robot and the environment.

A. Passive Training Strategy

Passive training requires no voluntary participation of patients, in which the robot tracks the predefined end-point trajectory carrying the affected limbs to take motion exercises. Impedance control aims to achieve active compliant behavior of the robot.

The controller architecture for passive training is shown in Fig. 3. L^{-1} represents inverse kinematics, and J^{-1} represents inverse of Jacobian matrix. τ_h is the vector of the sensed accidental contact torques between the robot and lower limbs in joint space, which can be converted into the force in Cartesian space coordinates, F, through the transposed inverse of Jacobian matrix, J^{-T}.

Since the velocity is changing rather slowly, the inertia term is omitted in impedance control. The effects of stiffness and damping terms are taken into account, related to K_1 and K_2 respectively, which both are diagonal coefficient matrices. Impedance control presents the position correction, X_f, and velocity correction, $\dot{X}_f$, to the reference trajectory in Cartesian space coordinates as

$$\begin{cases} X_f = K_1^{-1} J^{-T} \tau_h \\ \dot{X}_f = K_2^{-1} J^{-T} \tau_h \end{cases} . \tag{10}$$

Therefore, the end-point position command, X_c, and velocity command, $\dot{X}_c$, can be expressed as follow

$$\begin{cases} X_c = X_r + K_1^{-1} J^{-T} \tau_h \\ \dot{X}_c = \dot{X}_r + K_2^{-1} J^{-T} \tau_h \end{cases} \tag{11}$$

where X_r and $\dot{X}_r$ represent the reference end-point position and velocity respectively. The accidental torques generate end-point position and velocity adjustments to implement the active compliance of the rehabilitation robot, i.e. some position precision is given up to ensure the security and comfort for patients during training.

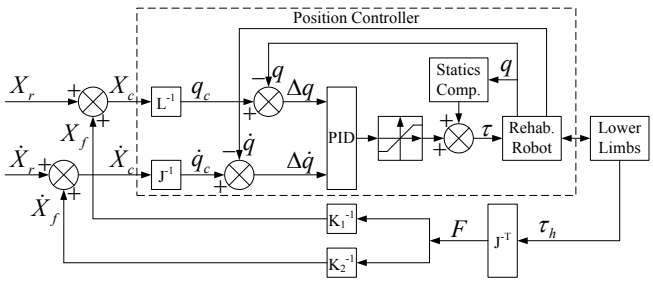

Fig. 3. Controller architecture for passive training

B. Damping-active Training Strategy

In damping-active training, voluntary participation of patients is required, and angular velocities of the robot joints are proportional to active joint torques, and impedance control presents the conversion formula.

The controller architecture for damping-active training is shown in Fig. 4. The outer impedance control loop is degraded into damping control, and the inner loop is a velocity controller. τ_h is the vector of the sensed active torques of hip joint and knee joint. B is a diagonal matrix of damping coefficients in impedance control. The given angular velocities of two joints are set to be zeros, $\dot{q}_r = [0\ 0]^T$, so the joint angular velocity commands, $\dot{q}_c$, equal to the angular velocity adjustments, $\dot{q}_f$, proportional to the feedback active torques in joint space as

$$\dot{q}_c = \dot{q}_f = B^{-1}\tau_h \tag{12}$$

which shows that more active joint torques are required to achieve higher angular velocities. The damping coefficients can be changed for different training resistances. The larger damping coefficients are, the more active torque contributions are needed to reach the same angular velocities.

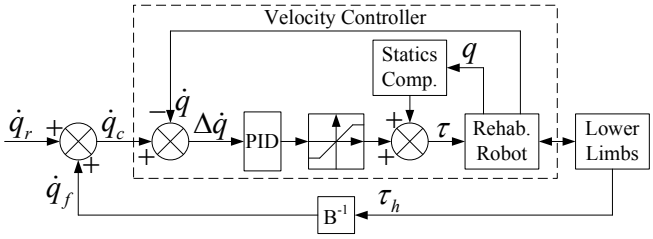

Fig. 4. Controller architecture for damping-active training

C. Spring-active Training Strategy

Spring-active training also requires voluntary participation of patients, in which the joint angular displacements are controlled by active joint torques, and the transformation is presented by impedance control as well.

The controller architecture for spring-active training is shown in Fig. 5. The outer impedance control loop is actually degraded into a stiffness controller, and the inner loop is position control. τ_h is the vector of the sensed active torques in joint space and K is the diagonal matrix of stiffness coefficients. The joint angular displacements are proportional to the active joint torques as

$$q_f = K^{-1}\tau_h. \tag{13}$$

The equilibrium angles of the two joints, q_r, are given as constants, accordingly, the joint angle commands, q_c, can be written as

$$q_c = q_r + K^{-1}\tau_h \tag{14}$$

which shows that larger angular displacements require more active joint torques, acting as an ideal spring model. Different training strengths can be achieved by changing the stiffness coefficients. Larger stiffness coefficients require more active torque contributions to reach the same angular displacements.

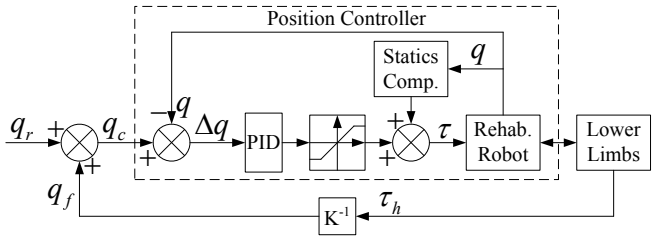

Fig. 5. Controller architecture for spring-active training

IV. Simulation Results and Discussion

The dynamics of the system shown in (8) is adopted as the system model in the simulation, with $D(q)$, $C(q,\dot{q})$ and $G(q)$ reduced by twenty percent compared to (5), (6) and (7). The friction and disturbance term is chosen as $T = K_r\dot{q}$, where $K_r = \text{diag}(1.2, 1.2)$. The following parameters are used in the simulation, $m_1 = 15.2$kg, $m_2 = 12.51$kg, $l_1 = 0.42$m, $l_2 = 0.41$m.

A. Passive Straining

Treadmill is employed in the simulation of passive training, and the desired end-point trajectory of the rehabilitation robot is predefined as

$$X_r = \begin{bmatrix} 0.63 + 0.1\cos(0.5\pi t) \\ 0.1\sin(0.5\pi t) \end{bmatrix}$$

which is a circle with the center as $(0.63,\ 0)$ and radius as 0.1m. The initial joint angles and angular velocities are chosen as $q_0 = [0.8\ \ -0.5]^T$ and $\dot{q}_0 = [0\ 0]^T$ respectively. Let stiffness and damping related diagonal matrices be $K_1 = \text{diag}(100, 100)$ and $K_2 = \text{diag}(100, 100)$ respectively. The unexpected contact torques in joint space between the robot and lower limbs are defined as

$$\tau_h = \begin{cases} [0\ \ 0]^T & 0 \le t < 6.5 \\ -5\dot{q} & 6.5 \le t \le 7 \\ [0\ \ 0]^T & 7 < t \le 10 \end{cases}.$$

Fig. 6 shows the simulation results of passive training in 10s. Trajectories of joints 1 and 2, as well as the end are shown in Fig. 6 (a), (b) and (c) respectively. During $6.5\text{s} \le t \le 7\text{s}$, obvious trajectory deviations appear because of the unexpected contact torques; thus, the compliant behavior is implemented, and some position precision is sacrificed to protect lower limbs from excessive interaction force. When the accidental contact torques vanish, the controller performs as a position controller.

B. Damping-active Training

In the simulation of damping-active training, the relationship between the active torques, τ_h, and angular displacements for the hip and knee joints of a lower limb are considered as ideal spring models, defined as

$$\tau_h = K_e(q_0 + K_e^{-1}\tau_0 - q)$$

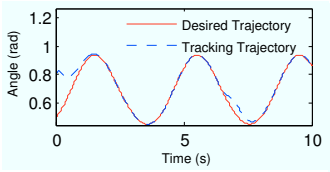

(a) Trajectory of joint 1

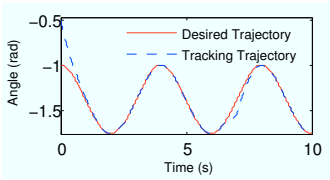

(b) Trajectory of joint 2

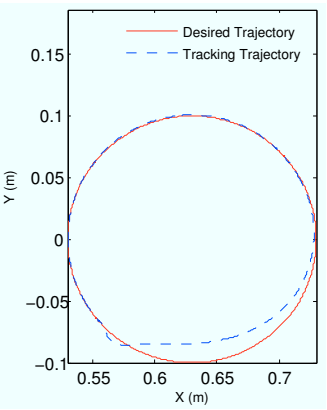

(c) Trajectory of the end, $6s<t<10s$

Fig. 6. Simulation results of passive training

where the diagonal matrix of joint stiffness coefficients is chosen as $K_e = \text{diag}(5, 5)$, the initial joint angles are $q_0 = [0.4 \ -0.4]^T$, and the initial input active torques are $\tau_0 = [2 \ -2]^T$.

The simulation results in 10s for joint 1 with $B = \text{diag}(3, 3)$ and $B = \text{diag}(5, 5)$ are shown in Fig. 7. Note that the unit of torques is different in the figures. It is verified that joint angular velocities are in proportion to active joint torques; thus, impedance control approach is feasible for damping-active training strategy. Compared Fig. 7 (a) with (b), larger damping coefficients leading to stronger training exercises has been proven. The simulation results for joint 2 performs similarly.

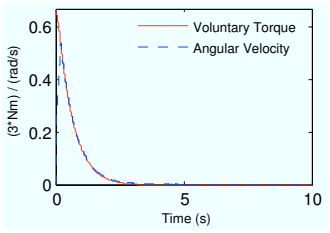

(a) Result of joint 1, B=diag$(3, 3)$

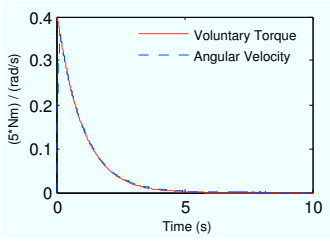

(b) Result of joint 1, B=diag$(5, 5)$

Fig. 7. Simulation results of damping-active training

C. Spring-active Training

In the simulation of spring-active training, the constant equilibrium joint angles are chosen as $q_r = [0.7 \ -1.3]^T$, the initial joint angular velocities are chosen as $\dot{q}_0 = [0 \ 0]^T$, and the active joint torques are defined as

$$\tau_h = \begin{cases} [0.5 \ -0.5]^T & 0 \le t < 2 \\ [2 \ -2]^T & 2 \le t < 4.5 \\ [-1.5 \ 1.5]^T & 4.5 \le t < 8 \\ [-1 \ 1]^T & 8 \le t \le 10 \end{cases}.$$

Fig. 8 shows the simulation results in 10s for joint 1 with $K = \text{diag}(5, 5)$ and $K = \text{diag}(10, 10)$. Note that the unit of torques is different in the figures. Joint angular displacements proportional to active torques have been implemented, and the feasibility of impedance control has been proven. Compared Fig. 8 (a) with (b), it is verified that the larger damping coefficients are, the more active joint torques are required to reach the same angular displacements. The performance of simulation results for joint 2 is similar.

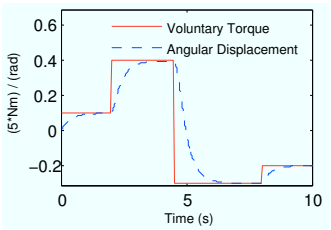

(a) Result of joint 1, K=diag$(5, 5)$

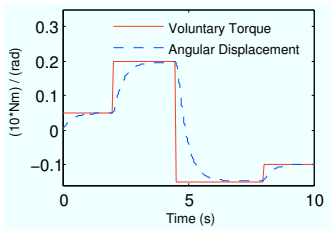

(b) Result of joint 1, K=diag$(10, 10)$

Fig. 8. Simulation results of spring-active training

V. Conclusion

Three training strategies for the lower limb rehabilitation robot applied to patients with paraplegia and hemiplegia have been accomplished using position-based impedance control. Better rehabilitation effect could be realized by selecting appropriate training strategies and impedance parameters depending on different patients and rehabilitation phases.

References

[1] M. Pohl, C. Werner, M. Holzgraefe, G. Kroczek, J. Mehrholz, I. Wingendorf, G. Holig, R. Koch and S. Hesse, Repetitive locomotor training and physiotheraphy improve walking and basic activities of daily living after stroke: a single-blind, randomized multicentretrial (DEutsche GAngtrainerStudie, DEGAS), *Clinical Rehabilitation*, vol. 21, pp. 17-27, 2007.

[2] M. Lotze, C. Braun, N. Birbaumer, S. Anders and L. G. Cohen, Motor learning elcited by voluntary, *Brain*, vol. 126, pp. 866-872, 2003.

[3] L. L. Cai, A. J. Fong, C. K. Otoshi, Y. Liang, J. W. Burdick, R. R. Roy and V. R. Edgerton, Implications of assist-as-needed robotic step training after a complete spinal cord injury on intrinsic strategies of motor learning, *Neurscience*, vol. 26, no. 4, pp. 10564-10568, 2006.

[4] Y. Yang, L. Wang, J. Tong and L. X. Zhang, Arm rehabilitation robot impedance control and experimentation, *IEEE International Conference on Robotics and Biomimetics*, pp. 914-918, Dec. 2006.

[5] E. G. Cao, Y. Inoue, T. Liu and K. Shibata, A sit-to-stand trainer system in lower limb rehabilitation, *International Conference on Advanced Intelligent Mechatronics*, pp. 116-121, Jul. 2011.

[6] A. Denève, S. Moughamir, L. Afilal and J. Zaytoon, Control system design of a 3-DOF upper limbs rehabilitation robot, *Computer Methods and Programs in Biomedicine*, vol. 89, no. 2, pp. 202-214, Feb. 2008.

[7] José L. Pons, *Wearable Robots: Biomechatronic Exoskeletons*, Chichester, West Sussex PO19 8SQ, England: John Wiley & Sons Ltd., 2008.

[8] M. W. Spong, S. Hutchinson and M. Vidyasagar, *Robot Dynamics and Control*, 2nd ed. USA: John Wiley & Sons Inc., Jan. 2004.

[9] S. Jung and T. C. Hsia, Neural network impedance force control of robot manipulator, *IEEE Transactions on Industrial Electronics*, vol. 45, no. 3, pp. 451-461, Jun. 1998.